Cell Transplantation, Vol. 16, pp. 229–244, 2007
Printed in the USA. All rights reserved.
Copyright © 2007 Cognizant Comm. Corp.

0963-6897/07 $90.00 + .00
E-ISSN 1555-3892
www.cognizantcommunication.com

Differential Loss of Presynaptic Dopaminergic Markers in Parkinsonian Monkeys

Diane T. Stephenson,* Mary Abigail Childs,* Qiu Li,† Santos Carvajal-Gonzalez,* Alan Opsahl,* Mark Tengowski,* Martin D. Meglasson,‡ Kalpana Merchant,§ and Marina E. Emborg¶

*Pfizer Global Research and Development, Groton, CT 06340, USA
†Schering Plough Research Institute, Cardiovascular Metabolic Disease, Kenilworth, NJ 07022-1300, USA
‡Ligand Pharmaceuticals, Discovery Research, San Diego, CA 92121, USA
§Eli Lilly, Neuroscience Division, Lilly Corporate Center, Indianapolis, IN 46285, USA
¶Wisconsin National Primate Research Center, Department of Anatomy, University of Wisconsin, Madison, WI 53715, USA

Assessment of dopamine nerve terminal function and integrity is a strategy employed to monitor deficits in Parkinson's disease (PD) patients and in preclinical models of PD. Dopamine replacement therapies effectively replenish the diminished supply of endogenous dopamine and provide symptomatic benefit to patients. Tyrosine hydroxylase (TH), dopamine transporter (DAT), vesicular monoamine transporter 2 (VMAT2), and amino acid decarboxylase (AADC) are widely used markers of dopaminergic neurons and terminals. The present studies were initiated to: (a) assess alterations in all four markers in the MPTP primate model of dopaminergic degeneration and (b) to determine whether L-DOPA treatment may itself modulate the expression of these markers. MPTP treatment induced a significant decline of dopaminergic immunoreactive fiber and terminal density in the basal ganglia. The amount of reduction varied between markers. The rank order of presynaptic marker loss, from most to least profound reduction, was TH > VMAT2 > DAT > AADC. Semiquantitative image analysis of relative dopaminergic presynaptic fiber and terminal density illustrated region-specific reduction of all four markers. Double immunofluorescence colocalization of two presynaptic markers on the same tissue section confirmed there was a more dramatic loss of TH than of VMAT2 or of DAT following MPTP treatment. L-DOPA treatment was associated with a significantly higher level of AADC and VMAT2 immunoreactivity in the caudate nucleus compared to placebo. These results illustrate that neurotoxic injury of the dopamine system in primates leads to altered and differential expression of presynaptic dopaminergic markers in the basal ganglia and that expression of such markers may be modulated by L-DOPA therapy. These findings have implications for the use of biomarkers of disease progression as well as for the assessment of neurorestorative strategies, such as cell replacement, for the treatment of PD.

Key words: Parkinson's disease; Tyrosine hydroxylase (TH); Vesicular monoamine transporter 2 (VMAT2); Dopamine transporter (DAT); Amino acid decarboxylase (AADC); L-DOPA; MPTP; Immunohistochemistry

INTRODUCTION

The discovery of extensive loss of dopamine (DA) in the striatum of parkinsonian patients led to the hypothesis that the decrease of striatal DA associated with dopaminergic nigral cells loss could be the cause of extrapyramidal symptoms in Parkinson's disease (PD) (15). Dopaminergic neurotoxicity in animals recapitulates many of the behavioral and pathological manifestations of human PD including akinesia, rigidity, tremor, postural instability, and degeneration of nigrostriatal neurons and loss of striatal dopamine (7). Primate models are unique in that they more faithfully mimic the behavioral aspects of PD compared to rodents. For example, L-DOPA induced dyskinesias are observed in primates but not observed in rodents treated with the dopaminergic neurotoxin *n*-methyl-4-phenyl-1,2,3,6-tetrahydropyridine (MPTP) (18). Additional evidence suggests that MPTP-treated primates also display striking similarities in pathologic profile compared to human PD (22,30). Although the MPTP model has limitations, such as difficulty mimicking nondopaminergic parkinsonian symptoms (3), MPTP-treated monkeys are considered well suited for evaluating PD therapies, especially cell re-

Address correspondence to Diane T. Stephenson, Ph.D., Pfizer Global Research and Development, Eastern Point Rd., Groton, CT 06340, USA. Tel: 860-686-6919; Fax: 860-686-0557; E-mail: Diane.t.Stephenson@pfizer.com

placement strategies (39). Characterization of presynaptic markers of monoaminergic neurotransmission is one approach to help understand the pathophysiology of PD models as well as illuminating endpoints that might be amenable to restorative therapies.

DA biosynthesis, like that of all catecholamines in the nervous system, originates from the essential amino acid precursor tyrosine. The rate-limiting step for DA biosynthesis is the conversion of L-tyrosine to L-dihydrophenylananine (L-DOPA) by the enzyme tyrosine hydroxylase (TH) (5). L-DOPA is subsequently converted to DA by L-aromatic amin oacid decarboxylase (AADC). In mammalian brain the highest concentration of AADC activity is found in the corpus striatum (28) mostly within the terminal ramifications of nigrostriatal neurons (34). The brain vesicular monoamine transporter 2 (VMAT2) is present also on dopaminergic neuronal terminals where it accumulates DA from the neuronal cytoplasm into synaptic vesicles (9,14,19,27). Normal vesicular DA release through calcium-dependent vesicle fusion with presynaptic membranes requires intact function of VMAT2 (12). DA nerve terminals also possess high-affinity DA uptake sites termed DA transporters (DAT), which are important in terminating transmitter action in the synapse and in maintaining transmitter homeostasis. Uptake is accomplished by a membrane carrier that is capable of transporting DA in either direction, depending on the existing concentration gradient (44). Because each marker represents a uniquely distinct aspect of dopaminergic function, evaluation of multiple markers is a powerful approach to understanding alterations in dopamine neurotransmission under conditions of a disease or pharmacotherapy.

Because of their key role for normal DA function, TH, AADC, DAT, and VMAT2 have been used as markers of presynaptic dopamine function biochemically, histologically in postmortem tissue, as well as in vivo in animal models and in human subjects. Studies in the postmortem brain of PD patients and in animal models of PD using neurochemistry (7,43), receptor autoradiography (47), and immunohistochemistry (31) demonstrate that the expression and function of dopaminergic markers is substantially reduced. In vivo, dopaminergic function has been assessed using PET or SPECT neuroimaging tracers that target these presynaptic markers (4). Although radiotracer imaging is widely used in PD patients, its use to establish disease modification by pharmacotherapeutic strategies remains controversial (36,42). The controversy stems from the potential of both disease- and treatment-induced adaptive changes in the level or function of the presynaptic markers in the injured nigrostriatal dopaminergic system. Indeed, one pivotal study in PD patients compared three PET neuroimaging tracers—[^{11}C]methylphenidate for DAT, [^{18}F]fluorodopa for AADC, and [^{11}C]dihydrotetrabenazine for VMAT2—with scans performed on the same day (26). The authors concluded that there are unique and differential compensatory changes in presynaptic dopaminergic nerve terminals in PD basal ganglia.

Animal models of PD present an opportunity to assess simultaneously and systematically changes in presynaptic dopaminergic markers within the same animal. With few exceptions, most previous studies have reported alterations in one or two markers in the same animal and not always under conditions of treatment with dopaminergic agents. Furthermore, although the effects of MPTP on nigrostriatal dopamine terminals is well established, little is known about the regional effects of MPTP treatment on dopamine innervations in various anatomic subdivisions of the striatum. Hence, in the present study, we investigated the expression of four presynaptic dopaminergic markers (TH, DAT, VMAT2, and AADC) by immunohistochemistry in subdomains of the basal ganglia of naive and MPTP-treated squirrel monkeys. Additionally, we investigated the effects of an L-DOPA treatment on relative presynaptic dopaminergic fiber and terminal density expression using a dosing regimen that clearly ameliorated extrapyramidal motor deficits induced by MPTP as well as produced dyskinesias (40). A comprehensive study describing the effects of MPTP neurotoxicity on behavioral outcome as a function of dopaminergic therapies has been previously described in the squirrel monkeys used in the present study (40,41).

MATERIALS AND METHODS

The primates in this study comprise a subset of animals used in an experiment to evaluate the effects of dopamine agonists compared to L-DOPA therapy in MPTP-treated squirrel monkeys (40). The experimental design is illustrated in Figure 1 (40).

Animals

Sixteen male squirrel monkeys (*Saimiri sciureus*), approximately 6 years of age, were pair housed with a 12-h light cycle. The treatment groups were naive ($n = 4$), MPTP + placebo ($n = 4$), and MPTP + L-DOPA ($n = 8$). All animals received water ad libitum. New World Monkey Chow was provided fresh each morning (4 h prior to behavioral testing) and supplied ad libitum. Diet was supplemented with fruit juice, PrimaBurger, Primate Chews, fresh vegetables, wheat bread, canned or fresh fruit, crackers, and cookies. The study was performed in accordance with federal guidelines of proper animal care and with the approval of and in compliance with the institutional IACUC.

MPTP Treatment

Twelve monkeys were administered MPTP subcutaneously 1–2 times per week to elicit a parkinsonian syn-

drome. Four additional animals remained untreated and were used as naive controls for morphology. Prior to each dosing each monkey was evaluated for its tolerance to MPTP and motor disability score. Individual doses and the total number of doses administered were titrated to produce similar degrees of parkinsonian disability (0.2–2.3 mg/kg, total accumulated dose 12.9–15.9 mg/kg). The number of individual doses ranged from 4 to 17 doses based on the above-mentioned criteria. Treatment duration ranged over a period of 4–5 weeks for the most sensitive monkeys (4 doses) and 18 weeks for the least sensitive monkeys (17 doses). The total number of MPTP doses was (mean ± SEM) L-DOPA group, 11.3 ± 1.3 and placebo group, 12.5 ± 1.6. Cumulative doses were L-DOPA group, 12.5 ± 2.0 mg/kg and placebo group, 12.4 ± 1.8 mg/kg. There were no significant differences between placebo and L-DOPA-treated monkeys for the number of doses of MPTP and total amount of MPTP. Hand feeding, subcutaneous fluid administration, and additional heating were provided as needed.

Drug Treatment

All monkeys were trained to be gently restrained by gloved hand and dosed at 12-h intervals by oral administration. Starting at 1 month after the end of the MPTP dosing, MPTP-treated monkeys received placebo (empty gelatin capsule) ($n = 4$) or L-DOPA (12.5 mg/kg) + carbidopa (1.5 mg/kg) ($n = 8$) bid. This dose of L-DOPA + carbidopa was chosen based on prior findings that the dose is maximally effective and consistently produces dyskinesias in MPTP-treated squirrel monkeys (25). The duration of treatment was 8 weeks.

Tissue Preparation

Three hours after the last oral L-DOPA or placebo dose, monkeys were euthanized by administration of a lethal dose of barbiturate. Animals were perfused transcardially with phosphate-buffered saline (PBS) followed by 2% periodate lysine paraformaldehyde fixative. Brains were fixed overnight at 4°C and then rinsed in PBS. The brains were cryoprotected through a series of graded solutions, 13% sucrose in PBS for 2 days, 15% sucrose in PBS for 2 days, and 18% sucrose in PBS for 3 days. The blocks were then frozen in dry ice-cooled isopentane and tissue blocks were stored at −80°C. Cryosections (20 μm thick) were collected onto charged slides (Superfrost Plus, VWR) using a Leica CM3050 cryostat. For each animal, three different coronal levels of the basal ganglia were collected with two sections per slide. The three levels corresponded to precommissural (A14.0), anterior commissure (A12.75), and postcommissural (A10.0); "A" refers to AP reference coordinates from a stereotaxic atlas of the squirrel monkey brain (8). A total of 32 serial sections were collected at each of the three levels and matched individually for each monkey using precise anatomical landmarks. Cryosections were stored at −80°C until staining.

Immunohistochemistry

The following antibodies were used: TH (anti-tyrosine hydroxylase monoclonal antibody ascites, 1:800, Chemicon International, Temecula, CA; polyclonal antibody anti-tyrosine hydroxylase, 1:1000, Calbiochem); AADC (rabbit anti-dopa decarboxylase, 1:200, Chemicon); VMAT2 (rabbit anti-vesicular monoamine transporter 2, 1:200, Chemicon); DAT (rat anti-dopamine transporter monoclonal antibody, 1:500, Chemicon). Each of the listed antibodies was used to stain the basal ganglia. These antibodies have been well described in the literature (17,48). Negative controls were included in each experimental run, which consisted of mouse IgG isotype control or rabbit IgG of a titer similar to that of the primary antiserum.

The methods for immunohistochemistry and tissue processing have been described previously (40). All groups of animals were stained in parallel as "sets" of tissue. A set was constituted by one slide from each anatomic level from each animal. Slides comprising a complete set were removed from −80°C and allowed to thaw for 10 min prior to staining. The slides were postfixed in 4% paraformaldehyde on wet ice for 10 min. The staining procedure was run on an automated Dako autostainer (DakoCytomation, Carpinteria, CA) as follows. Slides were rinsed with PBS, then incubated for 10 min with 0.1% H_20_2 in dH_20 to block endogenous peroxidase, followed by PBS rinses. Slides were blocked in 5% denatured goat serum for 10 min, followed by incubation in primary antibody for either 1 h (TH) or 24 h (VMAT2, DAT, AADC). Sections were labeled with anti-mouse or anti-rabbit Envision + polymer horseradish peroxidase (HRP) (DakoCytomation) for 30 min followed by development in diaminobenzidine (DAB). To enhance DAB reaction, the slides were incubated with DAB Enhancer (DakoCytomation). For sections containing the substantia nigra (SN), immunostained sections were lightly counterstained with hematoxylin to delineate cytoarchitecture/cellular structure.

One representative section from each level of all monkeys was also stained with cresyl violet for assessment of regions, landmarks, and overall tissue integrity. One set of sections from the SN levels was stained with H&E as well.

Quantification of Fibers/Terminal Density in the Basal Ganglia

The relative density of presynaptic dopaminergic fibers and terminals in the caudate and putamen was quantified using computer-assisted image analysis techniques. Quantification of the area of immunoreactive (ir) fibers and terminals in the basal ganglia was performed

using ImagePro software (MediaCybernetics, Silver Spring, MD). Immunoperoxidase stained sections using antibodies directed to presynaptic DA markers (TH, VMAT2, AADC, DAT) were analyzed by an investigator who was blinded to experimental treatment groups. Images were captured in black and white 8-bit monochrome with a 10× objective using a Spot RT camera. Matched anatomic regions were captured from each animal using reference landmarks and digital images were captured under the same exposure settings. Three rostrocaudal levels were examined from one brain hemisphere (randomly selected) of each one of the 16 monkeys. A total of six images were captured from each of level representing the dorsolateral, central, and ventromedial aspects of the caudate and the putamen. The total number of measurements per monkey was nine fields in the caudate and nine fields in the putamen per animal. The density of fibers and terminals was determined in fixed regions measuring 1000×1000 μm^2 as pixel area using a threshold level that was kept constant across all of the images. The signal in the white matter was subtracted as background. The pixels were converted to square microns using a calibration tool that utilized a stage micrometer. The final numeric value represented the area occupied by specific immunoreaction product represented as μm^2. A mean value was calculated for each subregion at each coronal level and a total mean was determined for each experimental group. The number of measurements for each animal included dorsolateral caudate nucleus ($n = 3$), central caudate nucleus ($n = 3$), and ventromedial caudate nucleus ($n = 3$) (mean of each region determined) and dorsolateral putamen ($n = 3$), central putamen ($n = 3$), and ventromedial putamen ($n = 3$) (mean of each region determined). Mean values ± SEM are represented in Figures 3 and 4. Tables 2 and 3 include both SEM and SD. The percent reduction of each marker was determined as percent loss in MPTP-treated animals compared to the value in naive controls.

Colocalization

Double immunofluorescence techniques were employed to investigate the distribution of two presynaptic dopaminergic markers simultaneously on the same tissue section. TH was compared directly to the distribution of either DAT (TH + DAT) or of VMAT2 (TH + VMAT2). AADC was not used for double staining because the antibody did not yield a good enough signal-to-noise ratio for optimal immunofluorescence detection. Immunohistochemistry was performed using colocalization of two antibodies, derived from different species, on the same tissue section by sequential double immunofluorescence techniques. Immunohistochemistry conditions were optimized for each antibody on individual single stained sections prior to dual staining. Control sections were stained with individual antibodies where one of the two antibodies was replaced with isotype control IgG from the appropriate species. Individual fluorophores and filter sets were chosen to eliminate the possibility of overlap of signal. The antibodies used were: TH polyclonal antibody + DAT monoclonal antibody and TH monoclonal + VMAT2 polyclonal antibodies. Each antibody was labeled by sequential incubations. Briefly, one antibody (monoclonal TH or DAT) was incubated overnight on sections in a humidified chamber. The following day, the primary mouse monoclonal antibody was labeled with anti-mouse-conjugated FITC (Antibodies Inc, 1:100 in PBS) in the dark for 1–3 h. After washing, the sections were incubated in the second primary antibody overnight and labeled with biotinylated anti-rabbit followed by avidin-Texas Red. Fluorescent-stained slides were washed and mounted in Vectashield (Vector Labs, Burlingame, CA) mounting medium containing DAPI (4′,6-diamidino-2-phenylindole), a nuclear counterstain. Slides were examined and digital photomicrographs taken on a Nikon E800 microscope equipped with epifluorescence and Nomarski optics.

Confocal Imaging

Images were acquired on a LSM510 confocal microscope (Carl Zeiss, Thornwood, NY) with a 63× Plan-apochromat 1.4 numerical aperture lens. FITC fluorescence was imaged using a 488 nm argon laser for excitation and a 505–550 nm bandpass emission filter. Texas Red fluorescence was imaged using a 543 nm helium-neon laser for excitation and a 560 nm longpass emission filter. DAPI fluorescence was imaged with a 364 nm argon laser for excitation and a 385–470 nm bandpass emission filter. Each fluorescent image through its specific channel was acquired individually and then merged using the Zeiss LSM5 software. Immunofluorescence of two presynaptic dopaminergic markers was assessed in single sections from two to three representative naive and MPTP + placebo-treated monkeys. Texas Red, FITC, and UV filters provided visualization of immunostaining compared to DAPI-stained nuclei in the same microscopic field.

Quantitative image analysis of individual digitally acquired confocal fluorescent images was performed using Image Pro Plus software (MediaCybernetics, Silver Spring, MD). A single field from a matching region was acquired from a representative naive and MPTP-treated animal stained with either TH + DAT or TH + VMAT2. For this analysis, the area of specific staining within the green channel or the red channel was assigned a pixel value in the naive and MPTP-treated conditions. The area of overlap (yellow) was also measured in the merged image and likewise assigned a pixel value. By comparing the pixel values of red, green, and yellow

channels in naive compared to MPTP-treated monkey, the percent reduction of each marker was calculated for each of the markers in the double stained section.

Statistical Analysis

Descriptive statistics of quantitative data for dopaminergic fiber and terminal density in the ventromedial, central, and dorsolateral subregions of the caudate and the putamen as a function of treatment group were computed. For each region (i.e., putamen and caudate), the dopaminergic fiber and terminal density were analyzed using a mixed model that included terms for subregion, animal within subregion (random effect), treatment, and treatment by animal within subregion (random effect). The comparisons were MPTP + placebo and MPTP + L-DOPA to naive, and MPTP + placebo to MPTP + L-DOPA, at each subregion level (i.e., ventromedial, central, and dorsolateral subregions of each rostrocaudal level). The pairwise estimated differences between treatments were calculated for each subregion using a significance level of $p < 0.05$. Additionally, the percent reduction of each presynaptic dopaminergic marker as a function of treatment was calculated by comparing the mean values of naive and treatment group monkeys within each nucleus.

RESULTS

MPTP-induced deficits in squirrel monkeys were assessed by both behavioral and pathologic criteria, thus providing validation of the model. MPTP administration produced a stable parkinsonian deficit that was ameliorated by L-DOPA treatment. L-DOPA therapy also induced the occurrence of dyskinesia and dystonia in MPTP-treated animals with a rapid onset and sustained duration (41). In all MPTP-treated animals, significant neurodegeneration of the substantia nigra pars compacta was observed and consisted of loss of Nissl substance, reduced TH immunoreactivity, and astrocytosis. Quantitative analyses were not performed in the substantia nigra.

Presynaptic Dopamine Markers

The distribution of presynaptic dopaminergic markers in the basal ganglia from naive monkeys consisted of a dense matrix of staining throughout the neuropil in the caudate and putamen (Fig. 1). In MPTP-treated primates, a distinctive reduction of immunoreactivity for all four dopaminergic markers (TH, VMAT, DAT, and AADC) was observed in both caudate and putamen (Figs. 1 and 2). Unexpectedly, not all DA markers appeared to be reduced to the same extent. By visual inspection of the stained sections, it appeared that some presynaptic dopaminergic markers were more profoundly reduced than others. TH-ir showed the most dra-

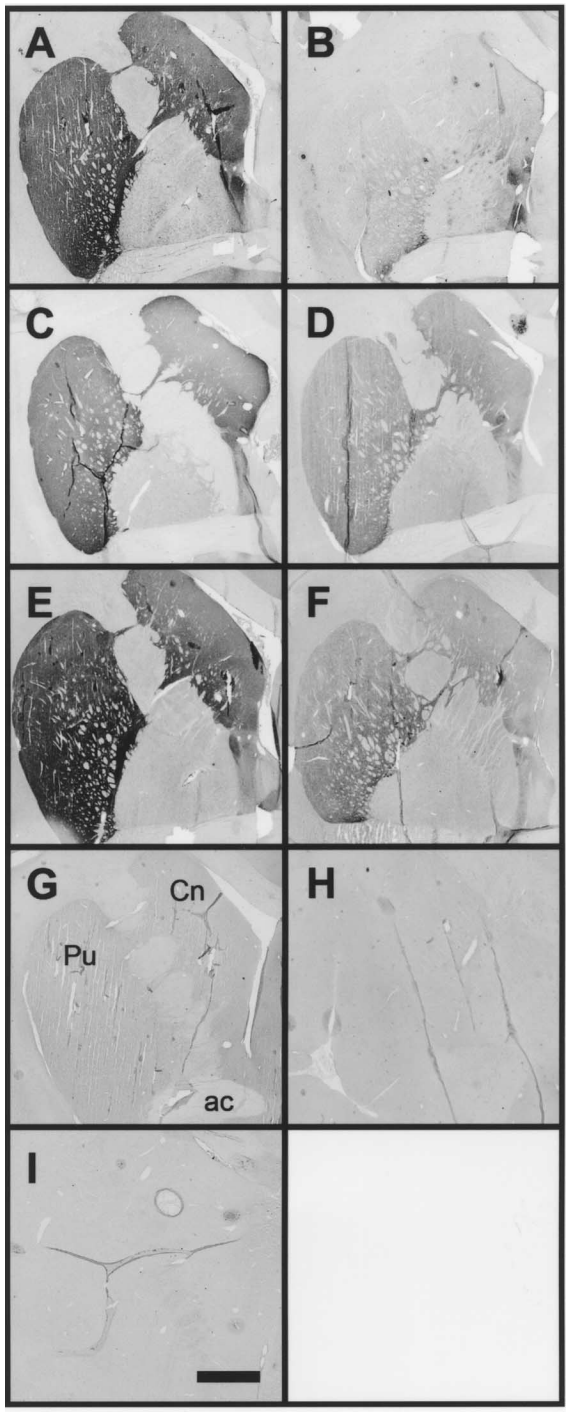

Figure 1. Expression of four presynaptic dopaminergic markers in basal ganglia of naive and MPTP treated primates. Low magnification illustration of immunoperoxidase staining of four presynaptic DA markers (A, B: TH; C, D: DAT; E, F: VMAT2; G, H: AADC) in hemibrains of a representative naive (left panels) and MPTP + placebo-treated monkey (right panels). The region highlights caudate (Cd) and putamen (Pu) at the level of the anterior commissure (ac) in image shown (G). (I) Adjacent section stained with mouse IgG isotype control antibody. Scale bar: 1.5 mm.

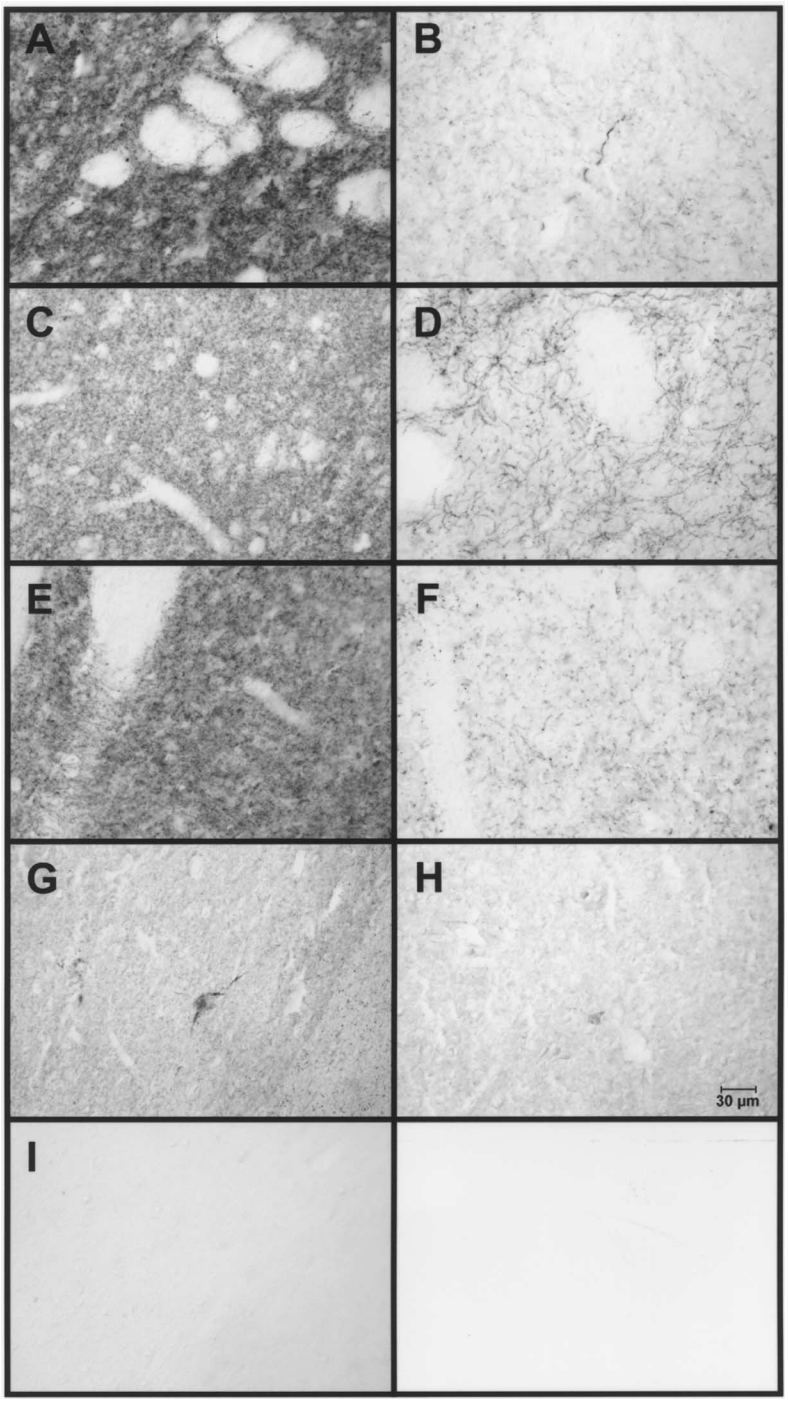

Figure 2. Expression of four presynaptic dopaminergic markers in naive and MPTP-treated putamen. High magnification illustration of immunoperoxidase staining of four presynaptic DA markers (A, B: TH; C, D: DAT; E, F: VMAT2; G, H: AADC) in the putamen of a representative naive (left panels) and MPTP + placebo-treated monkey (right panels). In naive brain, strong labeling of neuropil was observed with TH, DAT, and VMAT2 antibodies (A, C, E). Following MPTP treatment, fine individual neuropil threads and varicosities remained in both caudate and putamen (B, D, F). A more diffuse staining pattern was observed with AADC antibodies including rare immunoreactive neuronal cell bodies (G). Immunoreactivity of all four markers was visibly reduced in MPTP-treated primates. Nonspecific staining as assessed with isotype control antibody was completely negative (I). Scale bar: 30 µm (H).

matic reduction in the striatum of all MPTP-treated monkeys. VMAT2-ir was also substantially reduced in MPTP-treated primates (Fig. 1E, F) while DAT-ir (Fig. 1C, D) and AADC-ir (Fig. 1G, H) were reduced, but to a lesser extent. The differential reduction of presynaptic DA markers could be observed at both low (Fig. 1) and high (Fig. 2) magnifications. Immunoreactive fibers and nerve terminals in addition to rare neuronal cell bodies was observed; labeled neurons were more prominent in the ventromedial putamen with VMAT2, TH, and DAT antibodies. AADC-ir consisted of labeling of both individual somata and neuropil that was above background, consistent with previous reports (29). However, the overall intensity was much less than that observed with TH, VMAT2, and DAT antibodies, likely a function of antibody affinity/avidity. In summary, by qualitative assessment of immunostained sections, the overall rank of loss as a function of the lesion, from most to least profound reduction, was TH > VMAT2 > DAT > AADC.

To assess the relative magnitude of presynaptic loss in basal ganglia, a comprehensive semiquantitative analysis was undertaken on all immunoperoxidase stained sections. Table 1 demonstrates the relative reduction of each marker in the caudate and the putamen while Tables 2 and 3 highlight the values based on anatomic subdomains of caudate and putamen. Differential loss of presynaptic dopaminergic markers was observed in all monkeys following MPTP treatment. TH-ir fiber and terminal density was most profoundly reduced following MPTP lesion (92% caudate, 93% putamen; placebo vs. naive) (Table 1). The expression of DAT-ir was significantly reduced by 79% in the caudate and 76% in the putamen in MPTP + placebo versus naive monkeys (Table 1). VMAT2 expression was significantly reduced by 90% in the caudate and 88% in the putamen in MPTP placebo-treated versus naive monkeys (Table 1). AADC-ir displayed the least substantial reduction in fiber and terminal density with values of 39% decrease in the caudate and 36% decrease in the putamen in MPTP-treated versus naive monkeys (Table 1). To further refine the analyses, image analysis results were assessed by anatomic subregions of caudate and putamen. In all subregions, the degree of reduction of AADC was consistently less than the other three markers (Tables 2 and 3). TH and VMAT2 were most profoundly reduced as a function of MPTP treatment while DAT reduction was intermediary. Figs. 3 and 4 illustrate graphically the relative reduction of dopaminergic markers in MPTP-lesioned primates treated with placebo or L-DOPA. In virtually all subregions of both caudate (Fig. 3) and putamen (Fig. 4), a statistically significant reduction of dopaminergic markers as a function of MPTP treatment was observed. As we have previously described for TH (41), there was an anatomic gradient of immunoreactivity sections in MPTP-treated monkeys with the dorsolateral portion of the putamen showing the most dramatic loss and the ventromedial portion of the putamen showing some detectable TH-ir fibers and terminals. This anatomic gradient was similarly observed with the other antibodies in both caudate and putamen (Figs. 3 and 4, Tables 2 and 3).

Table 1. Effect of MPTP and L-DOPA Treatment on Relative Reduction of Presynaptic Dopaminergic Markers in Primate Basal Ganglia

	MPTP + Vehicle		MPTP + L-DOPA	
Marker	Caudate	Putamen	Caudate	Putamen
TH	92%	93%	87%	84%
DAT	79%	76%	69%	70%
AADC	39%	36%	18%*†	34%
VMAT2	90%	88%	80%†	81%

The data are expressed as percent reduction of immunoreactive fiber and terminal density (immunoperoxidase-stained sections) relative to naive. A total of nine microscopic fields of caudate and putamen obtained from three rostrocaudal levels were quantified in each animal. The values from three subregions of the caudate and the putamen were averaged to yield a single mean value for each region.
*Not significantly different from naive.
†Significantly different from vehicle, $p < 0.05$.

The effect of L-DOPA treatment on presynaptic marker fiber and terminal density in parkinsonian monkeys compared to placebo treatment was assessed in the caudate and putamen. The distribution and rank order of loss of markers in MPTP animals treated with L-DOPA was similar to the MPTP + placebo group (Tables 1, 2, 3, Figs. 3, 4). However, in the caudate nucleus, expression of VMAT2 and AADC was significantly elevated in MPTP + L-DOPA-treated primates compared to MPTP + placebo treatment (VMAT2, $p < 0.01$; AADC, $p < 0.05$) (Table 1). In fact, AADC-ir in the caudate of L-DOPA-treated animals was not significantly different from naive controls. In contrast, the putamen did not show significant differences between L-DOPA-treated and placebo groups in relative expression of any dopaminergic marker.

To confirm that there was differential loss of specific DA markers as a function of MPTP treatment, we compared two different markers on the same tissue section using double immunofluorescence colocalization and confocal laser scanning microscopy. Colocalization of TH and DAT (Fig. 5A) and of TH and VMAT2 (Fig. 5C) in the basal ganglia of naive monkeys revealed almost complete colocalization of the two markers (Fig. 5A, C: yellow or orange, arrows). These data confirm

Table 2. Effect of MPTP and L-DOPA Treatment on Presynaptic Dopaminergic Markers in Anatomic Subregions of Caudate in Primate Brain

		TH				DAT				AADC				VMAT2			
Treatment	Regions	Mean	SD	SEM	% Red	Mean	SD	SEM	% Red	Mean	SD	SEM	% Red	Mean	SD	SEM	% Red
No Lesion (i.e., naive)	dorsolateral	17277	12291	3548		58627	44984	12986		54603	25049	7231		64233	37211	10742	
	central	48655	26509	7653		51075	43773	12636		77737	26349	7606		83824	35471	10240	
	ventromedial	88478	38671	11163		68666	40832	11787		93140	24298	7014		107121	35244	10174	
MPTP + placebo	dorsolateral	931	1106	333	94.6	6092	7827	2360	89.6	33389	21926	6611	38.9	4480	6316	1904	93.0
	central	2297	2626	792	95.3	12415	12389	3735	75.7	43777	19496	5878	43.7	4824	6431	1939	94.2
	ventromedial	8816	7365	2221	90.0	16312	11337	3418	76.2	60634	23503	7086	34.9	14675	15179	4577	86.3
MPTP + L-DOPA	dorsolateral	2430	5091	1039	85.9	12627	12095	2522	78.5	46844	20337	4151	14.2	11473	12855	2624	82.1
	central	4418	5943	1213	90.9	17942	15574	3247	64.9	64005	22948	4684	17.7	14818	17051	3480	82.3
	ventromedial	13597	13176	2690	84.6	25176	19697	4107	63.3	70311	26145	5337	24.5	22781	23843	4867	78.7

The data are expressed as mean area (in square microns), SEM, SD, and percent reduction of immunreactive fiber and terminal density (immunoperoxidase-stained sections) compared to naive. A total of nine microscopic fields of caudate obtained from three rostrocaudal levels were quantified in each animal. Because the number of animals were different with the various groups, the number of measurements per region in the naive group was $n = 12$, for the MPTP + placebo group, $n = 11$, and for the MPTP + L-DOPA group, $n = 24$.

Table 3. Effect of MPTP and L-DOPA Treatment on Presynaptic Dopaminergic Markers in Anatomic Subregions of Putamen in Primate Brain

		TH				DAT				AADC				VMAT2			
Treatment	Regions	Mean	SD	SEM	% Red	Mean	SD	SEM	% Red	Mean	SD	SEM	% Red	Mean	SD	SEM	% Red
No lesion (i.e., naive)	dorsolateral	50571	43296	12499		88018	47783	13794		52603	24455	7060		86859	37977	10963	
	central	54753	23770	6862		93392	44510	12849		68548	28036	8093		100378	36608	10568	
	ventromedial	52078	28865	8333		91698	31330	9044		71745	22869	6602		113677	36620	10571	
MPTP + placebo	dorsolateral	777	1507	454	98.5	10764	8944	2697	87.8	35951	16958	5113	31.7	5946	9816	2960	93.2
	central	2597	4317	1302	95.3	23920	20764	6261	74.3	36747	14819	4468	46.4	4214	13123	3957	95.8
	ventromedial	5881	6893	2078	88.7	27152	9039	2725	70.4	49614	19332	5829	30.8	20796	23731	6851	81.7
MPTP + L-DOPA	dorsolateral	2035	2684	548	96.0	15795	13907	2900	82.1	39094	15945	3255	25.7	11875	11840	2417	86.3
	central	5777	7363	1503	89.4	23948	17693	3689	74.4	42029	14818	3025	38.7	19072	15229	3109	81.0
	ventromedial	19251	30749	6277	63.0	43335	25415	5299	52.7	45829	11120	2270	36.1	22868	20013	4085	79.9

The data are expressed as mean area (in square microns), SEM, SD, and percent reduction of immunreactive fiber and terminal density (immunoperoxidase-stained sections) compared to naive. A total of nine microscopic fields of putamen obtained from three rostrocaudal levels were quantified in each animal. Because the number of animals were different with the various groups, the number of measurements per region in the naive group was $n = 12$, for the MPTP + placebo group, $n = 11$, and for the MPTP + L-DOPA group, $n = 24$.

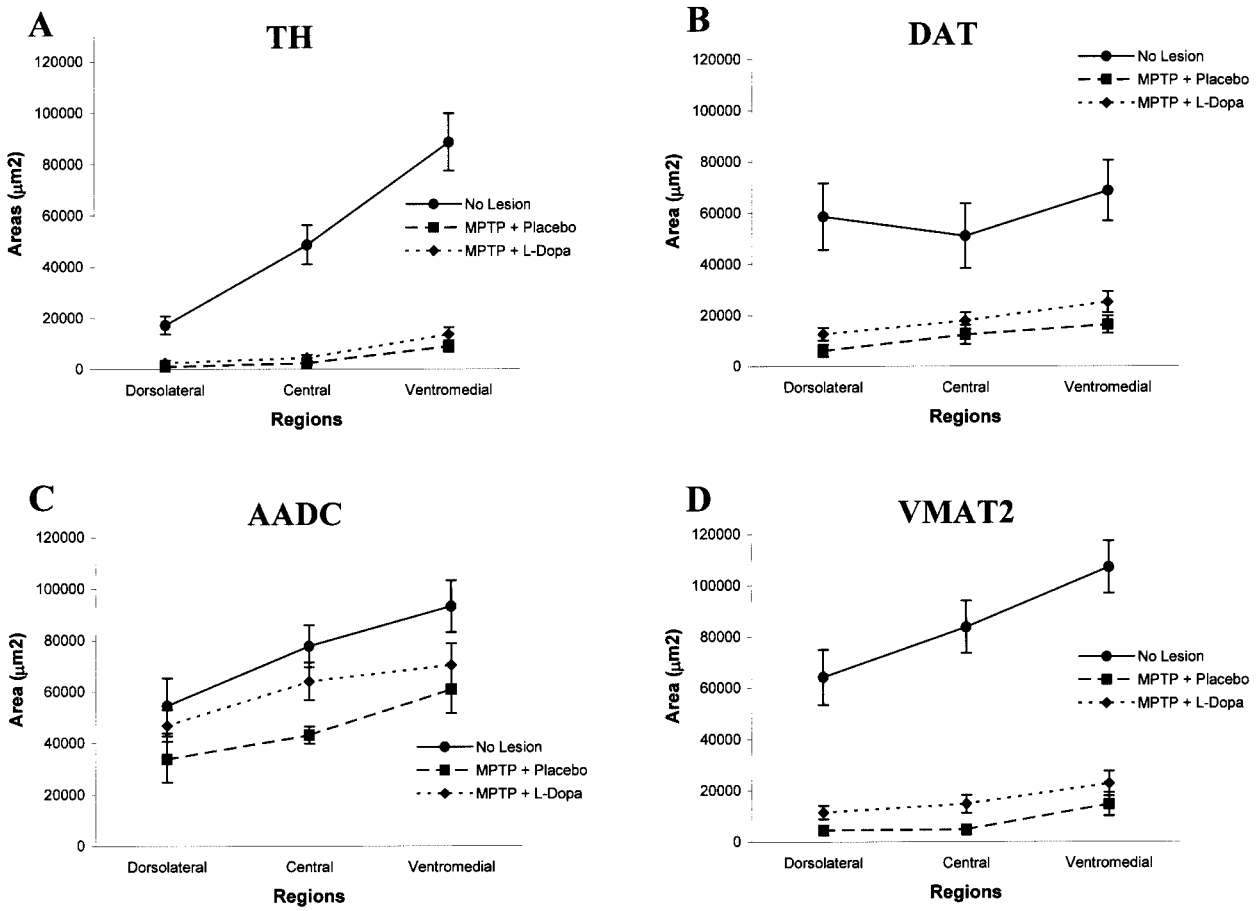

Figure 3. Semiquantitative image analysis of fiber and terminal density of four presynaptic dopaminergic markers in caudate nucleus from naive and MPTP-lesioned monkeys treated with and without L-DOPA therapy. Quantification of presynaptic dopaminergic marker immunoreactivity (A: TH; B: DAT; C: AADC; D: VMAT2) in the caudate of naive and MPTP + placebo and MPTP + L-DOPA-treated primates. The values represent the area of specific immunoreactivity (in square microns) derived from anatomic subregions of the caudate and putamen of immunoperoxidase stained sections. Values represent mean ± SEM from all primates within each treatment group. Individual values are expressed in Tables 2 and 3. Statistically significant reductions in fiber and terminal density in naive versus MPTP groups was observed with all four markers in all subregions with the exception of AADC (dorsolateral and central subregions); MPTP + L-DOPA versus naive, all subregions, NS. No significant differences were observed between area of fiber and nerve terminal immunoreactivity in subregions of MPTP + placebo compared to MPTP + L-DOPA treatments.

that the presynaptic dopaminergic markers assessed under conditions used here colocalize in normal brain. Similar to what was observed with immunoperoxidase staining (Figs. 1, 2), there was a distinctive reduction of TH-ir, DAT-ir, and VMAT2-ir in caudate and putamen in all MPTP-treated monkeys compared to naive monkeys (compare Fig. 5A with B and C with D; note similar size of blue nuclei). However, in sections from MPTP-treated animals, there were substantially fewer TH-ir fibers and terminals than DAT-ir fibers and terminals (i.e., more green than red structures) (Fig. 5B, arrowheads). This observation was consistent in both caudate and putamen. Likewise, more VMAT2-ir fibers and terminals were present in the caudate and putamen of MPTP-treated monkeys than TH-ir fibers and terminals in the same tissue section (Fig. 5D). Quantification of the changes in the representative field shown in Figure 3 by image analysis revealed a 62% reduction of DAT expression (green channel) and a 76% reduction of TH (red channel) (Fig. 5A vs. B). For VMAT2 + TH (Fig. 5C, D), a 65% reduction of the red channel (VMAT2) and a 91% reduction of the green channel (TH) following MPTP treatment was observed. Collectively, these data illustrated both qualitatively and quantitatively that presynaptic markers were differentially reduced as a function of MPTP treatment.

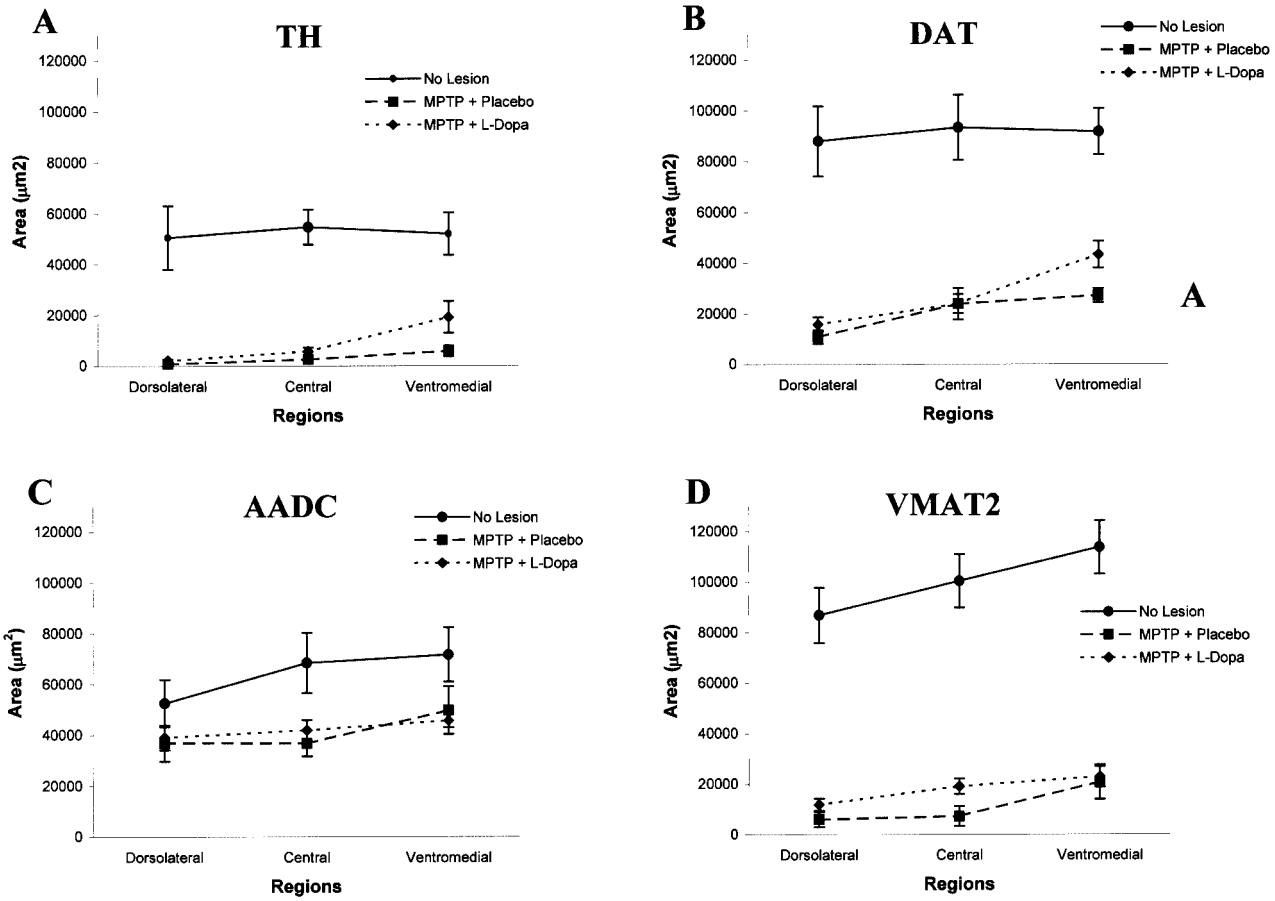

Figure 4. Quantification of presynaptic dopaminergic marker immunoreactivity (A: TH; B: DAT, C: AADC; D: VMAT2) in the putamen of naive and MPTP + placebo- and MPTP + L-DOPA-treated primates. Statistically significant reductions in fiber and terminal density in naive versus MPTP groups was observed with all four markers in all subregions with the exception of AADC (dorsolateral subregion). No significant differences were observed in MPTP + L-DOPA versus MPTP + placebo treatment in any subregion.

DISCUSSION

Our results indicate that MPTP-induced neurotoxicity produces an uneven loss of presynaptic dopaminergic markers in the nigrostriatal DA pathway in squirrel monkeys and that L-DOPA administration may modulate protein expression of a subset of the markers under conditions of dopamine depletion. Qualitatively, there was a dramatic reduction in immunoreactivity of all four presynaptic dopaminergic markers as a function of MPTP treatment. In addition, there were visible differences in the degree of dopaminergic nerve terminal loss among the different markers. The relative rank order of presynaptic marker loss, from most to least profound reduction, was TH > VMAT2 > DAT > AADC. Differential alterations in four presynaptic markers induced by MPTP was determined using qualitative and quantitative assessment of multiple immunoperoxidase stained sections as well as immunofluorescent colocalization of two markers in the same tissue section. To minimize any potential sources of error and to control for inherent variability in the assay, several experimental procedures were implemented including precise anatomic matching of three rostrocaudal levels of the basal ganglia, performing immunohistochemistry of all animals in parallel, and conducting image analysis using defined algorithms in a blinded fashion (e.g., images acquired with same exposures and image analysis conducted using a constant threshold by an individual blinded to the treatment groups). Furthermore, confidence in the data is substantiated by the fact that similar results were obtained using both peroxidase and fluorescent immunohistochemical techniques, including simultaneous staining of two markers on the same tissue section.

The novel aspect of the present study is the analysis of multiple dopaminergic markers, several of which are

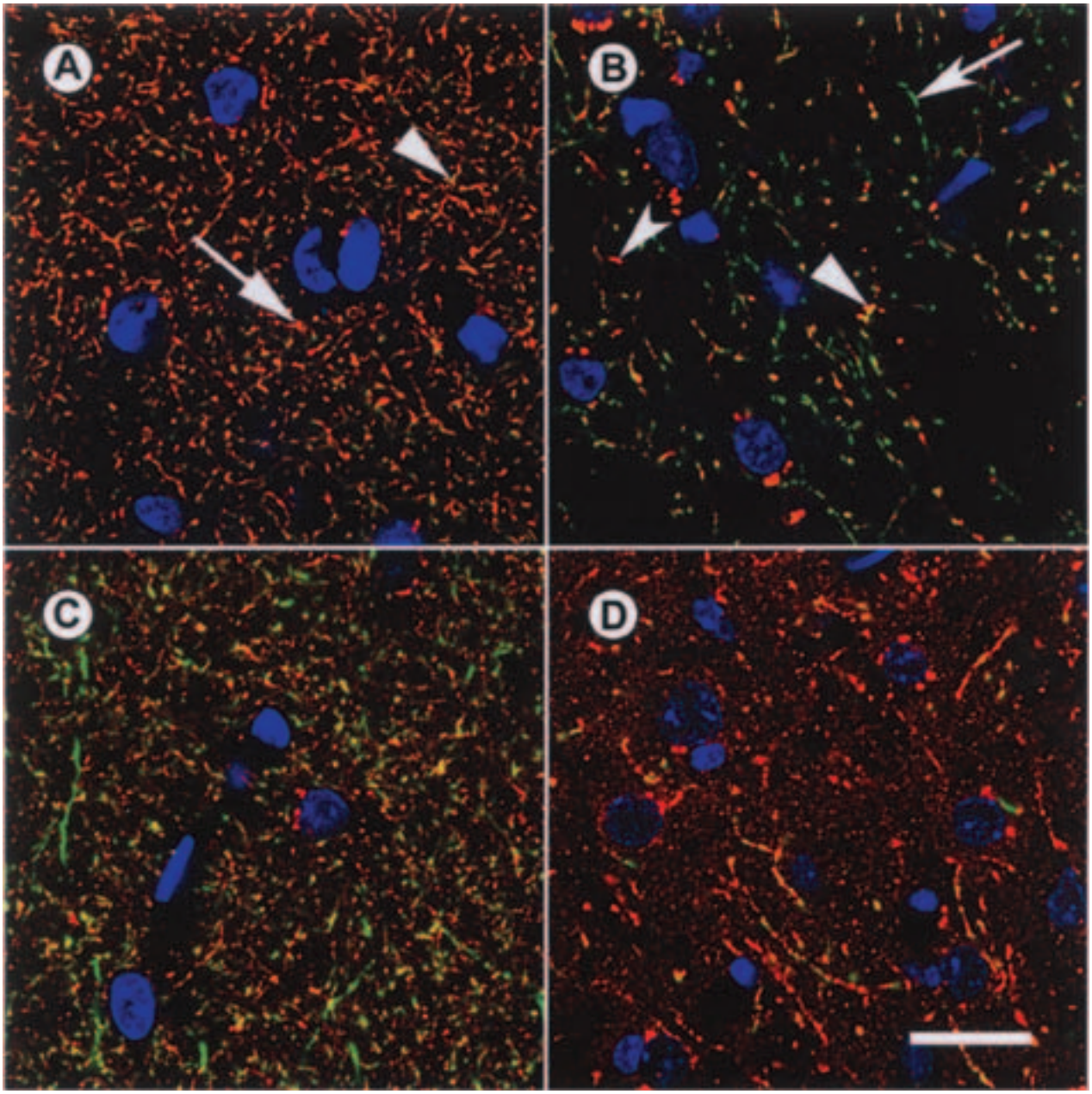

Figure 5. Confocal microscopy of two presynaptic markers colocalized on the same section in naive and MPTP-treated primate brain. Colocalization of two presynaptic dopaminetgic markers in the putamen (anterior commissure level) of a representative naive (A, C) and MPTP + placebo-treated (B, D) primate. Confocal microscopic images illustrate immunofluorescent staining of TH (red) plus DAT (green) (A, B) and VMAT2 (red) plus TH (green) (C, D). Neuronal nuclei were localized using DAPI (blue). Note distinctive reduction in all markers with MPTP treatment (compare B with A and D with C); yet, DAPI-stained nuclei are the same size in all fields. In naive brain, a near complete overlap of TH and DAT (A) and of VMAT2 and TH (C) positive fibers and terminals is observed (A: yellow, arrowhead; orange, arrow). Following MPTP treatment, there is a greater loss of TH than DAT {B: more green (concave arrow) than red (concave arrowhead)} and of TH than VMAT2 (D: more red than green) positive fibers/terminals. Quantification of each channel revealed a 76% reduction of TH (A vs. B, red), 62% reduction in DAT (A vs. B, green) while there was a 78% reduction in both TH + DAT double positive fibers and terminals (A vs. B, yellow). For VMAT2 and TH, a 65% reduction in VMAT2 (C vs. D, red), 91% reduction in TH (C vs. D, green), and a 88% reduction in both TH + VMAT2 double positive fibers and terminals (C, D, yellow) was found in the illustrated confocal images. Scale bar: 20 μm.

targets of clinical neuroimaging studies, to assess MPTP neurotoxicity and modulation by chronic L-DOPA therapy in nonhuman primates. The power of such an approach is the ability to investigate different aspects of dopaminergic functional integrity with unique markers, which when taken collectively conveys the overall function of dopaminergic neurons. Most investigators evaluate one (most commonly TH) or, in some studies, two markers of the DA system (17,20) in preclinical models of DA toxicity. One study in mice (43) reported that moderate doses of MPTP led to similar reductions in DA, DAT, VMAT2, and TH, the latter three of which were evaluated by immunohistochemical methods. The apparent discrepancy between our findings and this report include factors such as MPTP dosing regimes (chronic in the present study vs. acute MPTP treatment paradigm in the mouse study), time after MPTP treatment, age of animals, quantification methods, and, most importantly, species differences in responses to MPTP.

Data in both animal models as well as in human PD subjects using other experimental assays support the hypothesis that there is differential loss of presynaptic dopaminergic markers with lesions of the dopamine system. For example, rapid and differential loss of DAT and VMAT2 radioligand binding has been demonstrated in MPTP-treated mice (21). Using immunocytochemistry, Jakowec et al. (17) demonstrated that TH and DAT differ in expression following recovery from MPTP in mice. AADC activity has been reported to be reduced to a lesser extent than TH activity in a rodent model of PD (13) and in patients with PD (32). Furthermore, parkin knockout mice show reduced levels of DAT and VMAT2 but not TH (16). In primates, there is limited information in which multiple markers of the dopaminergic system are evaluated in the same study. Neurochemical measures of striatal dopamine loss in rhesus monkeys has shown that the interregional pattern of dopamine loss in the striatum is not identical to that in PD; there is an equal reduction in striatal dopamine loss in both caudate and putamen following MPTP treatment whereas in idiopathic PD, the caudate nucleus is less affected by DA loss as compared to the putamen (35). Differential effects on nigral DAT versus TH expression in postmortem primate brain has been reported with aging (7). Most recently, a neuroimaging study in primates illustrated a differential reduction of three neuroimaging tracers of monoaminergic terminals following aging and MPTP treatment (6). Interestingly, the VMAT2 selective radiotracer [^{11}C]DTBZ was reportedly the most sensitive indicator of MPTP-induced dopamine depletion in striatum compared to the DAT radiotracer, [^{11}C]methylphenidate, and the DOPA decarboxylase tracer, [^{18}F]DOPA. These results using noninvasive methods are consistent with the present findings using pathology with regard to the differential magnitude of reduction for the markers as well as the expression of VMAT2 relative to other markers.

In PD patients, neuroimaging using sensitive radiotracers of the DA system have revealed that alterations in one marker do not necessarily overlap with those of another marker. Lee and colleagues (26) compared striatal positron emission tomography (PET) scans using [^{11}C]dihydrotetrabenazine (DTBZ; labeling VMAT2), [^{11}C]methylphenidate (labeling DAT), and [^{18}F]DOPA (labeling mainly AADC). Their data led to the conclusion that the activity of AADC was upregulated whereas DAT was downregulated in the striatum of PD patients. These data are consistent with the present findings showing minimal reduction of AADC fiber and terminal density in MPTP-treated monkeys compared to DAT. Furthermore, postmortem studies of PD brains by Wilson and colleagues (47) have also shown unequal reduction in three different DA neuronal markers using biochemical, radioligand binding, and immunocytochemical methodologies. The authors found a less severe reduction of the DAT/VMAT2 radioligands relative to DA and DAT protein. Because most of the PD patients were treated with L-DOPA, the study could not rule out the possibility that pharmacologic treatment altered levels of the dopamine markers. Our results suggest that differential loss of DA markers itself occurs after nigrostriatal dopaminergic injury in the absence or presence of dopaminergic therapy. Although it is acknowledged that noninvasive imaging of DAT, which detects a functional end point (dopamine uptake), is not analogous to antigenic expression evaluated postmortem, one recent study demonstrates that DAT-ir significantly correlates with DAT imaging as assessed by SPECT (1). These data suggest that imaging presynaptic dopaminergic function and postmortem assessments of presynaptic dopaminergic markers may be comparable.

We report that a symptomatically efficacious L-DOPA treatment regimen that elicited persistent dyskinesias significantly increases AADC and VMAT2 expression in the caudate nucleus of MPTP-treated monkeys compared to placebo treatment. These results are novel in that AADC and VMAT2 have not been shown to be altered with short-term L-DOPA treatment in rodent model systems (29,45). In contrast, L-DOPA treatment produced a slight but statistically nonsignificant elevation of TH and of DAT fiber and terminal density compared to the vehicle group. Interestingly, chronic L-DOPA administration for 6 months to moderately 6-hydroxydopamine-lesioned rats induces a partial recovery of TH, DAT, and VMAT2 in the denervated territories of the striatum, but this is not observed in severely depleted conditions (31). In our study, the extent and severity of the parkinsonian deficit was similar,

by behavioral criteria, in placebo and L-DOPA-treated animals at baseline, thus eliminating the possibility that differences in presynaptic terminal density could be attributed to different severity of the lesion prior to treatment (40). AADC preservation in the basal ganglia may represent a plastic mechanism to increase availability of DA to postsynaptic DA receptors. Our results suggest that L-DOPA treatment can further stimulate AADC production in remaining DA terminals as an adaptive response to increases in availability of its substrate, L-DOPA. To attribute the changes in AADC and VMAT2 specifically and definitively to L-DOPA treatment, a wash-out period following L-DOPA discontinuation would be necessary because the wash-out should reverse the changes in these markers. This was not carried out in the present study but is a strategy possible with noninvasive imaging and is employed in dopamine therapy clinical studies in human PD (33). Given that AADC and VMAT2 actively metabolize a variety of monoamines, the potential contribution of nondopaminergic mechanisms to the changes in AADC and VMAT2 expression are topics for future investigation.

Our results in monkeys of no significant change in DAT expression with L-DOPA treatment contrasts with the results of the clinical ELLDOPA study reported by Fahn et al. (10), who reported that L-DOPA treatment produced greater decline in [^{123}I]βCIT uptake than the placebo group. Although the DAT measurements were not identical between these two studies, evidence suggests that DAT immunoreactivity correlates with DAT uptake assessed by SPECT following MPTP (1). These apparent discrepant results require further investigation in both animal and clinical studies.

The clinical relevance of the nonhuman primate study is limited somewhat by the fact that the data represent a single time point following a defined set of MPTP and L-DOPA dosing conditions. This may not reflect what might occur after different durations of disease and/or treatments. Indeed, in MPTP-treated mice, presynaptic dopaminergic markers undergo time-dependent changes, and recovery of antigenicity is observed at later time points after certain acute treatment regimens (17). However, reversibility of MPTP-induced deficits (e.g., behavioral outcome) is more commonly observed in mice than in primates (7). The primates in this study were administered multiple MPTP doses over several months followed by at least 1-month recovery to achieve a stable parkinsonian state prior to administration of therapy. Analysis of the same endpoints at other time points would be important to assess whether the differential loss we report in this study changes at different time points post-MPTP or under different L-DOPA treatment conditions.

Overall, the results reported here are consistent with the dynamic regulation of nigrostriatal dopamine function, which makes it susceptible to adaptive changes during the course of the disease and/or treatment (46). Adaptive changes such as increased L-DOPA turnover (37) and receptor supersensitivity (dopamine D2 receptor upregulation) (2) are thought to overcome early dopamine deficits such that typical PD signs do not become manifest until a substantial deficit in nigrostriatal dopamine function develops (11). The present results illustrating differential loss of presynaptic dopamine markers is additional evidence of the pathologic similarities between the MPTP primate model and human PD. Postmortem PD brain studies report differential reduction of markers (47). By neuropathologic criteria, the resemblance of MPTP-treated primates to human PD includes nigrostriatal neurodegeneration (18,25), the presence of microglial activation (24,30), and α-synuclein expression (22,38). The present findings of changes in presynaptic dopaminergic markers provide further insights into the dynamic regulation of nigrostriatal dopamine function under conditions of dopaminergic degeneration. Furthermore, these results provide guidance for evaluating the effects of therapies on presynaptic dopaminergic markers in primate models and in human PD.

ACKNOWLEDGMENTS: The authors acknowledge Mark Connell for animal handling, dosing, and care and Carol A. Simmons for performing histology techniques. We also acknowledge Lynn Renish and Jeff Joyce for assistance with DAT staining protocols. This research was supported by Pfizer Global Research and Development. Dr. Emborg gratefully acknowledges the support by the Kinetics Foundation, NIH NINDS RO1-NS40578, and by NIH grant 5P51RR000167 the Wisconsin National Primate Research Center, University of Wisconsin—Madison.

REFERENCES

1. Andringa, G.; Drukarch, B.; Bol, J. G. J. M.; de Bruin, K.; Sorman, K.; Habraken, J. B. A.; Booij, J. Pinhole SPECT imaging of dopamine transporters correlates with dopamine transporter immunohistochemical analysis in the MPTP mouse model of Parkinson's disease. Neuroimage 26:1150–1158; 2005.
2. Antonini, A.; Schwarz, J.; Oertel, W. H.; Pogarell, O.; Leenders, K. L. Long term changes of striatal dopamine receptors in patients with Parkinson's disease: A study with positron emissoin tomography and [^{11}C]raclopride. Mov. Disord. 12:33–38; 1997.
3. Braak, H.; Ghebremedhin, E.; Rub, U.; Bratzke, H.; Del Tredici, K. Stages in the development of Parkinson's disease-related pathology. Cell Tissue Res. 318:121–134; 2004.
4. Brooks, D. J. Neuroimaging in Parkinson's disease. Neuro Rx 1:243–254; 2004.
5. Cooper, J. R.; Bloom, F. E.; Roth, R. H. Dopamine—the biochemical basis of neuropharmacology. New York: Oxford University Press; 1991:285–337.
6. Doudet, D. J.; Rosa-Neto, P.; Munk, O. L.; Ruth, T. J.; Jivan, S.; Cumming, P. Effect of age on markers for monoaminergic neuonrsl of normal and MPTP-lesioned rhesus monkeys; a multitracer PET study. Neuroimage 30: 26–35; 2006.

7. Emborg, M. E. Evaluation of animal models of Parkinson's disease for neuroprotective strategies. J. Neurosci. Methods 139:121–143; 2004.
8. Emmers, R.; Akert, K. A stereotaxic atlas of the brain of the squirrel monkey (*Saimiri sciureus*). Madison: University of Wisconson Press; 1963.
9. Erickson, J. D.; Eiden, L. E.; Hoffman, B. J. Expression cloning of a reserpine-sensitive vesicular monoamine transporter. Proc. Natl. Acad. Sci. USA 89:10993–10997; 1992.
10. Fahn, S.; the Parkinson Study Group. Does levodopa slow or hasten the rate of progression of Parkinson's disease? J. Neurol. 252:IV37–IV42; 2005.
11. Fearnley, J. M.; Lees, A. J. Ageing and Parkinson's disease: Substantia nigra regional selectivity. Brain 114: 2283–2301; 1991.
12. Gasnier, B. The loading of neurotransmitters into synaptic vesicles. Biochimie 82:327–337; 2000.
13. Hefti, F.; Melamed, E. Dopamine release in rat striatum after administration of L-dopa as studied with in vivo electrochemistry. Brain Res. 225:333–346; 1981.
14. Henry, J. P.; Botton, D.; Sagne, C.; Isambert, M. F.; Desnos, C.; Blanchard, V.; Reisman-Vozari, R.; Krejci, E.; Massoulie, J.; Gasnier, B. Biochemistry and molecular biology of the vesicular monoamine transporter from chromaffin granules. J. Exp. Biol. 196:251–262; 1994.
15. Hornykiewicz, O.; Kish, S. J. Biochemical pathophysiology of Parkinson's disease. Adv. Neurol. 45:19–34; 1986.
16. Itier, J. M.; Ibanez, P.; Mena, M. A.; Abbas, N.; Cohen-Salmon, C.; Bohme, G. A.; Laville, M.; Pratt, J.; Corti, O.; Pradier, L.; Ret, G.; Joubert, C.; Periquet, M.; Araujo, F.; Negroni, J.; Casarejos, M. J.; Canals, S.; Solano, R.; Serrano, A.; Gallago, E.; Sanchez, M.; Denefle, P.; Benavides, J.; Tremp, G.; Rooney, T. A.; Brice, A.; Garcia de Yebenes, J. Parkin gene inactivation alters behaviour and dopamine neurotransmission in the mouse. Hum. Mol. Genet. 12:2277–2291; 2003.
17. Jakowec, M. W.; Nixon, K.; Hogg, E.; McNeill, T.; Petzinger, G. M. Tyrosine hydroxylase and dopamine transporter expression following 1-methyl-4-phenyl-1,2, 3,6-tetrahydrpyridine-induced neurodegeneration of the mouse nigrostriatal pathway. J. Neurosci. Res. 76:539–550; 2004.
18. Jenner, P. The contribution of the MPTP-treated primate model to the development of new treatment strategies for Parkinson's disease. Parkinsonism Relat. Disord. 9:131–137; 2003.
19. Johnson, R. G. Accumulation of biological amines into chromaffin granules: A model for hormone and neurotransmitter transport. Physiol. Rev. 68:232–307; 1988.
20. Jourdain, S.; Morissette, M.; Morin, N.; DiPaolo, T. Oestrogens prevent loss of dopamine transporter (DAT) and vesicular monoamine transporter (VMAT2) in substantia nigra of 1-methyl-4-phenyl-1,2,3,6-tetrahydrpyridine mice. J. Neuroendocrinol. 17:509–517; 2005.
21. Kilbourn, M. R.; Kuszpit, K.; Sherman, P. Rapid and differential losses of in vivo dopamine transporter (DAT) and vesicular monoamine transporter (VMAT2) radioligand binding in MPTP-treated mice. Synapse 35:250–255; 2000.
22. Kowall, N. W.; Hantraye, P.; Brouillet, E.; Beal, M. F.; McKee, A. C.; Ferrante, R. J. MPTP induces alpha-synuclein aggregation in the substantia nigra of baboons. Neuroreport 11:211–213; 2000.
23. Langston, J. W.; Ballard, P. Parkinsonian induced by MPTP: Implications for treatment and the pathogenesis of Parkinson's disease. Can. J. Neurol. Sci. 11:160–165; 1984.
24. Langston, J. W.; Forno, L. S.; Tetrud, J.; Reeves, A. G.; Kaplan, J. A.; Karluk, D. Evidence of active nerve cell degeneration in the substantia nigra of humans years after 1-methyl-4-phenyl-1,2,3,6-tetrahydrpyridine exposure. Ann. Neurol. 46:598–605; 1999.
25. Langston, J. W.; Quik, M.; Petzinger, G.; Jakowec, M.; Di Monte, D. A. Investigating levodopa-induced dyskinesias in the parkinsonian primate. Ann. Neurol. 47:S79–89; 2000.
26. Lee, C. S.; Samii, A.; Sossi, V.; Ruth, T. J.; Schulzer, M.; Holden, J. E.; Wudel, J.; Pal, P. K.; de la Fuente-Fernandez, R.; Calne, D. B.; Stoessl, A. J. In vivo positron emission tomographic evidence for compensatory changes in presynaptic dopaminergic nerve terminals in Parkinson's disease. Ann. Neurol. 47:493–503; 2000.
27. Liu, Y.; Peter, D.; Roghani, A.; Schuldiner, S.; Privé, G. G.; Eisenberg, D.; Brecha, N.; Edwards, R. H. A cDNA that suppresses MPP^+ toxicity encodes a vesicular amine transporter. Cell 70:539–551; 1992.
28. Lloyd, K. G.; Hornykiewicz, O. Occurrence and distribution of aromatic L-amino acid (L-DOPA) decarboxylase in the human brain. J. Neurochem. 19:1549–1559; 1972.
29. Lopez-Real, A.; Rodriguez-Pallares, J.; Guerra, M. J.; Labandeira-Garcia, J. L. Localization and functional significance of striatal neurons immunoreactive to aromatic L-amino acid decarboxylase or tyrosine hydroxylase in rat parkinsonian models. Brain Res. 969:135–146; 2003.
30. McGeer, P. L.; Schwab, C.; Parent, A.; Doudet, D. Presence of reactive microglia in monkey substantia nigra years after 1-methyl-4-phenyl-1,2,3,6-tetrahydropyridine administration. Ann. Neurol. 54:599–604; 2003.
31. Murer, M. G.; Dziewczapolski, G.; Menalled, L. B.; Garcia, M. C.; Agid, Y.; Gershanik, O.; Raisman-Vozari, R. Chronic levodopa is not toxic for remaining dopamine neurons, but instead promotes their recovery, in rats with moderate nigrostriatal lesions. Ann. Neurol. 43:561–575; 1998.
32. Nagatsu, T.; Yamaguchi, T.; Rahman, M. K.; Trocewicz, J.; Oka, K.; Hirata, Y.; Nagatsu, I.; Narabayashi, H.; Kondo, T.; Iizuka, R. Catecholamine-related enzymes and the biopterin cofactor in Parkinson's disease and related extrapyramidal diseases. Adv. Neurol. 40:467–473; 1984.
33. Olanow, C. W.; Agid, Y.; Mizuno, Y.; et al. Levodopa in the treatment of Parkinson's disease: Current controversies. Mov. Disord. 19:997–1005; 2004.
34. Pate, B. D.; Kawamata, T.; Yamada, T.; McGeer, E. G.; Hewitt, K. A.; Snow, B. J.; Ruth, T. J.; Caine, D. B. Correlation of striatal fluorodopa uptake in the MPTP monkey with dopaminergic indices. Ann. Neurol. 34:331–338; 1993.
35. Pifl, C.; Schingnitz, G.; Hornykiewicz, O. The neurotoxin MPTP does not reproduce in the rhesus monkey the interregional pattern of striatal dopamine loss typical of idiopathic Parkinson's disease. Neurosci. Lett. 92:228–233; 1988.
36. Ravina, B.; Eidelberg, D.; Ahlskog, J. E.; Albin, R. L.; Brooks, D. J.; Carbon, M.; Dhawan, V.; Feigin, A.; Fahn, S.; Guttman, M.; Gwinn-Hardy, K.; McFarland, H.; Innis, R.; Katz, R. G.; Kieburtz, K.; Kish, S. J.; Lange, N.; Langston, J. W.; Marek, K.; Morin, L.; Moy, C.; Murphy, D.; Oertel, W. H.; Oliver, G.; Palesch, Y.; Powers, W.; Seibyl, J.; Sethi, K. D.; Shults, C. W.; Sheehy, P.; Stoessl, A. J.; Holloway, R. The role of radiotracer imaging in Parkinsons disease. Neurology 64:208–215; 2005.

37. Sossi, V.; de la Fuente-Fernandez, R.; Holden, J. E.; Schulzer, M.; Ruth, T. J.; Stoessl, J. Changes of dopamine turnover in the progression of Parkinson's disease as measured by positron emission tomography: Their relation to disease-compensatory mechanisms. J. Cereb. Blood Flow Metab. 24:869–876; 2004.
38. Spillantini, M. G.; Schmidt, M. L.; Lee, V. M.; Trojanowski, J. Q.; Jakes, R.; Goedert, M. Alpha-synuclein in Lewy bodies. Nature 388:839–840; 1997.
39. Soderstrom, K.; O'Malley, J.; Steece-Collier, K.; Kordower, J. H. Neural repair strategies for Parkinson's disease: Insights from primate models. Cell Transplant. 15: 251–265; 2006.
40. Stephenson, D. T.; Meglasson, M. D.; Connell, M. A.; Childs, M. A.; Hajos-Korcsok, E.; Emborg, M. E. The effects of a selective dopamine D2 receptor agonist on behavioral and pathologic outcome in MPTP-treated squirrel monkeys. J. Pharmacol. Exp. Ther. 314:1257–1286; 2005.
41. Stephenson, D. T.; Li, Q.; Simmons, C.; Connell, M. A.; Meglasson, M. D.; Merchant, K. M.; Emborg, M. E. Expression of GAD65 and GAD67 immunoreactivity in MPTP-treated squirrel monkeys with or without L-DOPA adminstration. Neurobiol. Dis. 20:347–359; 2005.
42. Suchowersky, O.; Gronseth, G.; Perlmutter, J.; Reich, S.; Zesiewicz, T.; Weiner, W. J. Practice parameter: Neuroprotective strategies and alternative therapies for Parkinson disease (an evidence-based review). Neurology 66: 976–982; 2006.
43. Tillerson, J. L.; Caudle, W. M.; Reverson, M. E.; Mille, G. W. Detection of behavioral impairments correlated to neurochemical deficits in mice treated with moderate doses of MPTP. Exp. Neurol. 178:80–90; 2002.
44. Uhl, G. R. Dopamine transporter: Basic science and human variation of a key molecule for dopaminergic function, locomotion, and parkinsonism. Mov. Disord. 18(Suppl. 7):S71–80; 2003.
45. Vander Borght, T.; Kilbourn, M.; Desmond, T.; Kuhl, D.; Frey, K. The vesicular monoamine transporter is not regulated by dopaminergic drug treatments. Eur. J. Pharmacol. 294:577–583; 1995.
46. Whone, A. L.; Moore, R. Y.; Piccini, P. P.; Brooks, D. J. Plasticity of the nigropallidal pathway in Parkinson's disease. Ann. Neurol. 53:206–213; 2003.
47. Wilson, J. M.; Levey, A. J.; Raiput, A.; Ang, L.; Guttman, M.; Shannak, K.; Niznik, H. B.; Hornykiewicz, O.; Pifl, C.; Kish, S. Differential changes in neurochemical markers of striatal dopamine nerve terminals in idiopathic Parkinson's disease. Neurology 47:718–726; 1996.
48. Witkovsky, P.; Veisenberger, E.; Haycock, J. W.; Akopian, A.; Garcia-Espana, A.; Meller, E. Activity-dependent phosphorylation of tyrosine hydroxylase in dopaminergic neurons of the rat retina. J. Neurosci. 24:4242–4249; 2004.